

# Ordered Alignment of CdS Nanocrystals on MWCNTs without Surface Modification

Bin Liu<sup>†</sup> and Jim Yang Lee<sup>\*,†,‡</sup>

Singapore–MIT Alliance and Department of Chemical and Biomolecular Engineering,  
National University of Singapore, 10 Kent Ridge Crescent, Singapore 119260

Received: October 27, 2005; In Final Form: November 18, 2005

This paper describes a facile hydrothermal procedure capable of aligning CdS nanocrystals on multiwalled carbon nanotubes (MWCNTs) without the use of organic bridging molecules such as cysteamine and carboxylates. The direct placement of CdS on MWCNTs allows good mixing and better interfacing between the two nanophases. The synthesis conditions can in principle be tuned to produce modulations in compositions, phases, and crystal orientations to the need of optoelectronic and photonic applications.

## Introduction

Studies on low dimensional nanostructured inorganic materials have gradually migrated from the past emphasis on the synthesis and arrangement of phase-pure building block materials<sup>1</sup> to constructing functional nanocomposites with tunable properties through composition, size and morphology control.<sup>2</sup> The organization of metal or semiconductor nanoparticles on carbon nanotubes (CNTs) is one good example motivated by the desire to combine the properties of two functional nanoscale materials to achieve a wider range of applications.<sup>3</sup> Most current methods of binding metal or semiconductor nanocrystals to CNTs<sup>4–9</sup> often make use of small organic bridging molecules to improve the adhesion between the nanocrystals and CNTs. This not only complicates the synthesis but also results in indirect and poorer contact between the different phases. The resulting increase in the barrier to electron transport can adversely affect the material performance in optoelectronic applications.<sup>10</sup>

CdS, with a band gap of 2.42 eV at room temperature, is a venerable II–VI semiconductor which finds applications in solar cells, light-emitting diodes, and sensors. CdS can be fabricated in a number of nanostructures such as nanodots, nanorods, and nanowires.<sup>11</sup> Very recently, cysteamine-protected CdS nanoparticles were coupled to CNTs with terminal carboxylate groups to produce photocurrents at unprecedented high quantum yields.<sup>12</sup> A facile hydrothermal procedure is reported here which is capable of aligning CdS nanocrystals on multiwalled carbon nanotubes (MWCNTs) without the need for organic bridging molecules such as cysteamine and carboxylates. The direct placement of CdS on MWCNTs allows good mixing and better interfacing between the two nanophases. The synthesis conditions can, in principle, be tuned to produce modulations in compositions, phases, and crystal orientations that are designed to enhance material performance in optoelectronic and photonic applications.

## Experimental Section

0.01–0.02 g of MWCNTs (Aldrich) was added to 20 mL of deionized water under ultrasonic irradiation for 30 min at room temperature to ensure good dispersion. 0.001 mol of  $\text{Cd}(\text{NO}_3)_2 \cdot 4\text{H}_2\text{O}$  and 0.001 mol of thiourea were then added successively under constant stirring, followed by 0–10 mL of ammonia solution (32% v/v) or 0–10 mL of ethylenediamine (EDA). The mixture was then transferred to a Teflon-lined stainless steel autoclave (custom-made cylinder with 4 cm cross-sectional diameter and 50 mL internal volume) and placed inside an electric oven at 100–180 °C for 2–18 h. After the synthesis, the solid product recovered by sedimentation was washed several times with deionized water and pure ethanol, and dried in vacuum. The crystal structure of the solid product was determined by powder X-ray diffraction (XRD, Shimadzu XRD-6000, Cu–K $\alpha$  radiation).<sup>13</sup> Morphological and compositional information of the solid product was obtained by field-emission scanning electron microscopy and energy-dispersive X-ray spectroscopy (FESEM/EDX, JSM-6700F), transmission electron microscopy and selected area electron diffraction (TEM/SAED, JEM-2010F), and high-resolution TEM (HRTEM, JEM-3010F). UV–visible absorption spectra were recorded on a Shimadzu UV-3010 PC scanning spectrometer using DI water as the reference.

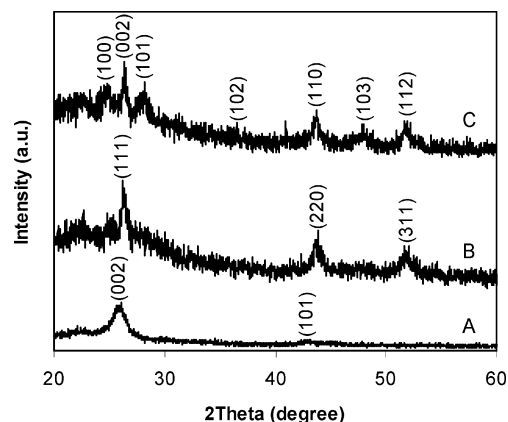
## Results and Discussion

Figure 1 shows the XRD patterns of MWCNTs and the CdS/MWCNT nanocomposites synthesized in ammonia and ethylenediamine, respectively. The diffraction pattern in Figure 1A agrees well with the (002) and (101) reflections of MWCNTs (at 26.3° and 44.7° respectively). Despite the overlap of diffraction peaks between MWCNTs and CdS, there are well-resolved non-MWCNT related signatures that indicate sufficiently good crystallinity of the CdS deposit (Figure 1B,C). All diffraction peaks in Figure 1B can be indexed to the cubic CdS phase with the lattice constant  $a = 5.82 \text{ \AA}$  (space group:  $F\bar{4}3m$ ; JCPDS card no. 10-0454) and those in Figure 1C can be indexed to the hexagonal CdS phase with the lattice constants  $a = 4.14 \text{ \AA}$  and  $c = 6.72 \text{ \AA}$ , respectively (space group:  $P6_3mc$ ; JCPDS card no. 41-1049).

\* To whom correspondence should be addressed. E-mail: cheleejy@nus.edu.sg.

<sup>†</sup> Singapore–MIT Alliance.

<sup>‡</sup> Department of Chemical and Biomolecular Engineering.



**Figure 1.** XRD patterns of (A) MWCNTs, (B) cubic phase CdS/MWCNT nanocomposite synthesized in ammonia, and (C) hexagonal phase CdS/MWCNT nanocomposite synthesized in ethylenediamine.

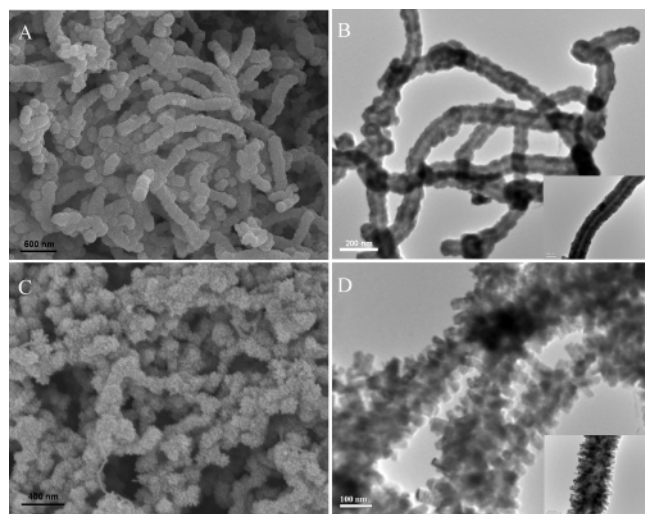


**Figure 2.** (A) FESEM and (B) TEM images of CdS/MWCNT nanocomposite synthesized in ammonia. Synthesis conditions: 0.02 g of MWCNTs + 20 mL of  $\text{H}_2\text{O}$  + 0.001 mol of  $\text{Cd}(\text{NO}_3)_2 \cdot 4\text{H}_2\text{O}$  + 0.001 mol of thiourea + 10 mL of ammonia at 180 °C for 18 h. (C) FESEM and (D) TEM images of CdS/MWCNTs synthesized in ethylenediamine. Synthesis conditions: 0.02 g of MWCNTs + 20 mL of  $\text{H}_2\text{O}$  + 0.001 mol of  $\text{Cd}(\text{NO}_3)_2 \cdot 4\text{H}_2\text{O}$  + 0.001 mol of thiourea + 5 mL of ethylenediamine at 180 °C for 18 h. Insets are high magnification TEM images.

Figure 2 shows that the two CdS/MWCNT nanocomposites are core-shell in structure. The CdS to MWCNT stoichiometry is 1:1 according to EDX measurements (Supporting Information, SI-1). The surface of the composite synthesized in ammonia was coated with a thin layer of CdS. The resulting thicker and rougher surface texture is distinctively different from the underlying MWCNT substrate (Supporting Information, SI-2). The strong contrast between the inner and outer regions along the CNT axis in the transmission electron microscopy (TEM) images in Figure 2B is characteristic of the formation of a coaxial structure. High resolution transmission electron microscopy (HRTEM, Figure 3) shows further that the external layer was composed of small CdS nanoparticles with an average diameter of 8 nm. Interestingly, when the synthesis was carried out in ethylenediamine instead of ammonia, the CdS deposit would grow preferentially along the CdS [001] direction (Figure 3) and aligned perpendicularly to the propagating axis of the CNTs (Figure 2C,D), forming a well-ordered heterostructure. The adhesion of the CdS shell to the MWCNT substrate was very strong and could not be detached from the latter, even after 1 h of sonication at room temperature.

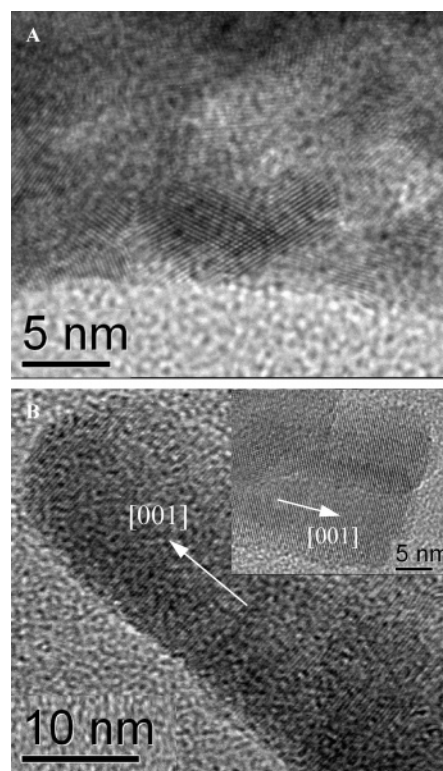


**Figure 3.** High-resolution transmission electron microscopy (HRTEM) images of (A) CdS/MWCNT nanocomposite synthesized in ammonia, (B) CdS/MWCNT nanocomposite synthesized in ethylenediamine.

The presence of ammonia or ethylenediamine was central to the formation of an aligned CdS structure on MWCNTs. Without ammonia or ethylenediamine, only large and discrete CdS microparticles were formed in the solution phase. It is well-known that ammonia or ethylenediamine could coordinate with  $\text{Cd}^{2+}$  to form chelating complexes.<sup>14</sup> Chelation would lead to the decrease of the  $\text{Cd}^{2+}$  concentration in the solution, facilitating the formation of smaller CdS nanocrystals. In addition, the cadmium chelating complexes are more likely to adsorb preferentially on the MWCNT walls, similar to their adsorption on glass.<sup>15</sup> The immobilization of cadmium complexes allows heterogeneous nucleation and growth to take place via a ligand exchange condensation reaction, with the  $\text{S}^{2-}$  released from the thermal decomposition of thiourea at elevated temperatures.

When the reaction time was reduced from 18 to 2 h, intermediate products in the form of necklace-like and MWCNT-aligned multipod nanoflowers were obtained (Figure 4 and Figure 5). The particles threading through the CNTs were of nearly the same size. Closer examination revealed that each of these particles was made up of many smaller nanoparticles, similar to those forming the external shell of the uniformly coated MWCNTs. The following hypothesis may be put forward: at the early stages of the reaction with the release of  $\text{S}^{2-}$  from thiourea, the CdS formation reaction occurred heterogeneously on selected sites on the external walls of the MWCNTs. The CdS nanoparticles formed were catalytic toward the decomposition of thiourea,<sup>16</sup> leading to the formation of clustered particles around the sites of action. The process of particle dissolution and recrystallization then began with the increase in reaction time, and a uniform layer was finally formed over the entire external MWCNT surface at steady state. The presence of ethylenediamine was instrumental in the process as it is an excellent chelating agent known for its ability to promote growth of one-dimensional nanomaterials.<sup>17</sup> It does so by adsorbing preferentially on certain crystallographic planes, thereby creating

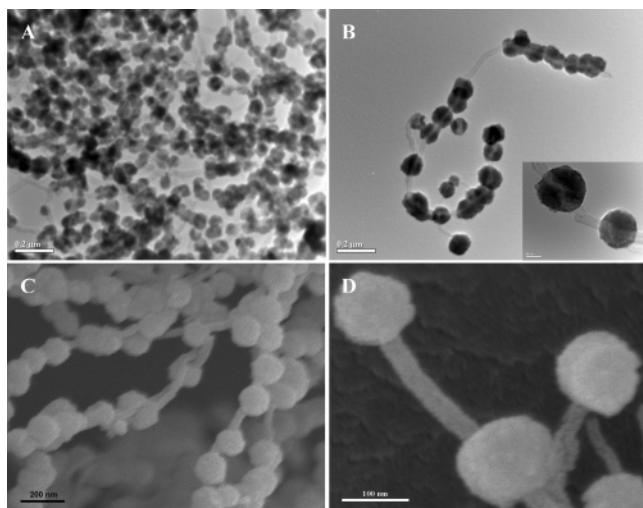


**Figure 4.** (A) and (B) TEM and (C) and (D) FESEM images of CdS/MWCNT nanocomposite synthesized in ammonia at short reaction times. Synthesis conditions: 0.02 g of MWCNTs + 20 mL of  $\text{H}_2\text{O}$  + 0.001 mol of  $\text{Cd}(\text{NO}_3)_2 \cdot 4\text{H}_2\text{O}$  + 0.001 mol of thiourea + 10 mL of ammonia at 180 °C for 2 h. Insets are high magnification TEM images.

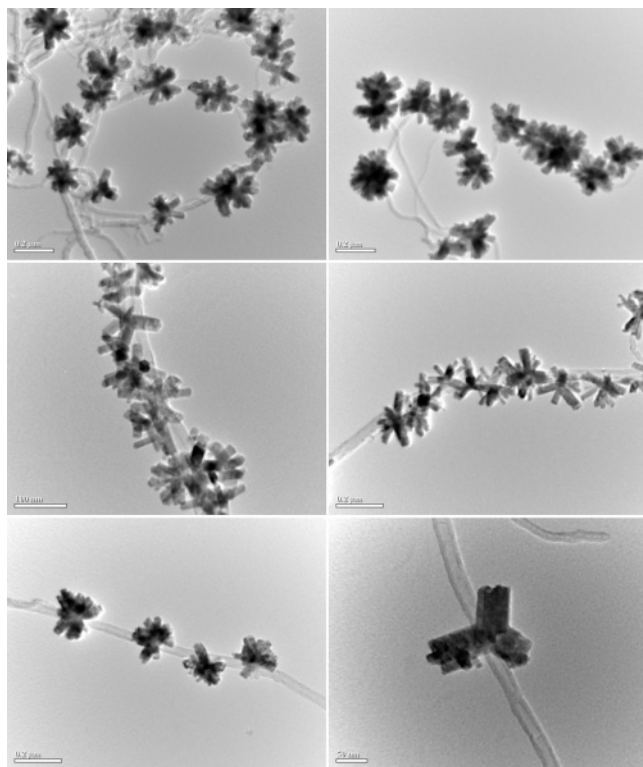


**Figure 5.** TEM images of CdS/MWCNT nanocomposite synthesized in ethylenediamine at short reaction times. Synthesis condition: 0.02 g of MWCNTs + 20 mL of  $\text{H}_2\text{O}$  + 0.001 mol of  $\text{Cd}(\text{NO}_3)_2 \cdot 4\text{H}_2\text{O}$  + 0.001 mol of thiourea + 5 mL of ethylenediamine at 180 °C for 2 h.

anisotropy in crystal growth. In the present case, the addition of ethylenediamine allowed CdS to grow preferentially in the CdS [001] direction. At short reaction times the deposition was limited to a few sparsely distributed multipod CdS nanoflowers on the MWCNT walls (Figure 5). Each of the branched nanorods was randomly oriented and had similar diameter and the same [001] growth direction. However, at longer reaction times the deposition of CdS seeds on the MWCNT walls would become random, and the continued growth of individual multipod CdS nanoflowers in the preferred directions would be physically hindered once the branches started to intercept one another. The

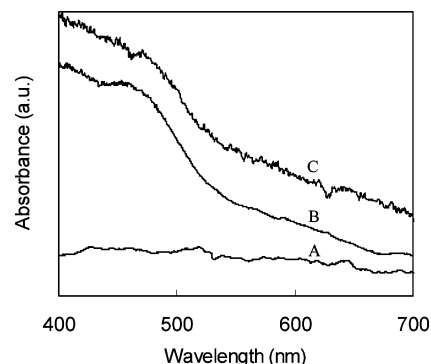


**Figure 6.** Absorption spectra of (A) MWCNTs in DI water, (B) CdS/MWCNT nanocomposite synthesized in ethylenediamine in DI water, and (C) CdS/MWCNT nanocomposite synthesized in ammonia in DI water.

suppression of directed crystal growth gave rise to layer densification and thickness buildup in the direction perpendicular to the axis of the CNTs.

The optical properties of the as-prepared CdS/MWCNT nanocomposites in the UV–visible region were measured. Figure 6 shows the absorption spectra of MWCNTs before and after the deposition of CdS nanocrystals. A stable suspension of the CdS/MWCNT composites in DI water could not be obtained during the measurements, and as a result some measurement noises are apparent in the spectra. The absorption spectrum of MWCNTs was rather featureless in the visible region. The absorption peak that emerged after the deposition of CdS particles was caused by the formation of CdS crystals on the MWCNT surface. Compared with the absorption by bulk CdS, a blue shift was observed, which indicates size quantization effects. A classical Tauc approach<sup>2k</sup> was used to estimate the optical band gap for the CdS nanocrystals on the MWCNT surface. The optical band gaps estimated as such were 2.52 eV and 2.42 eV for CdS nanocrystals synthesized in ethylenediamine and in ammonia, respectively.

## Conclusions

In summary, heterostructured CdS/MWCNT nanocomposites were synthesized by a facile hydrothermal method. Although the particle size of CdS on the MWCNTs could not be easily controlled, the surface coverage, the crystal phases, and the orientation could be altered by manipulating the reaction time and by selecting the appropriate chelating agent. The various interesting structures of CdS/MWCNT nanocomposites may be useful to nanoelectronics and photonics applications. The method of preparation is generic and can be easily adapted to the production of other metal sulfide coated MWCNT nanocomposites.

**Acknowledgment.** The present work is supported by Singapore–MIT Alliance.

**Supporting Information Available:** EDX patterns and TEM images. This material is available free of charge via the Internet at <http://pubs.acs.org>.

## References and Notes

- (1) (a) Velikov, K. P.; Christova, C. G.; Dullens, R. P. A.; van Blaaderen, A. *Science* **2002**, 296, 106–109. (b) Park, S.; Lim, J.-H.; Chung, S.-W.; Mirkin, C. A. *Science* **2004**, 303, 348–351. (c) Kovtyukhova, N. I.; Mallouk, T. E. *Chem.-Eur. J.* **2002**, 8, 4355–4363.
- (2) (a) van Bommel, K. J. C.; Friggeri, A.; Shinkai, S. *Angew. Chem., Int. Ed.* **2003**, 42, 980–999. (b) Zeng, H.; Li, J.; Liu, J. P.; Wang, Z. L.;



- Sun, S. *Nature* **2002**, 420, 395–398. (c) Redl, F. X.; Cho, K.-S.; Murray, C. B.; O'Brien, S. *Nature* **2003**, 423, 968–971. (d) Lauhon, L. J.; Gudiksen, M. S.; Wang, D.; Lieber, C. M. *Nature* **2002**, 420, 57–61. (e) Gudiksen, M. S.; Lauhon, L. J.; Wang, J.; Smith, D. C.; Lieber, C. M. *Nature* **2002**, 415, 617–620. (f) Wu, Y.; Fan, R.; Yang, P. *Nano Lett.* **2002**, 2, 83–86. (g) Urbach, A. R.; Love, J. C.; Prentiss, M. G.; Whitesides, G. M. *J. Am. Chem. Soc.* **2003**, 125, 12704–12705. (h) Mokari, T.; Rothenberg, E.; Popov, I.; Costi, R.; Banin, U. *Science* **2004**, 304, 1787–1790. (i) Manna, L.; Scher, E. C.; Li, L.-S.; Alivisatos, A. P. *J. Am. Chem. Soc.* **2002**, 124, 7136–7145. (j) Hong, B. H.; Bae, S. C.; Lee, C.-W.; Jeong, S.; Kim, K. S. *Science* **2001**, 294, 348–351. (k) Liu, B.; Zeng, H. C. *J. Phys. Chem. B* **2004**, 108, 5867–5874. (l) Yang, H. G.; Zeng, H. C. *J. Am. Chem. Soc.* **2005**, 127, 270–278.
- (3) (a) Daniel, M.-C.; Astruc, D. *Chem. Rev.* **2004**, 104, 293–346. (b) Tessler, N.; Medvedev, V.; Kazes, M.; Kan, S. H.; Banin, U. *Science* **2002**, 295, 1506–1508. (c) Planeix, J. M.; Coustel, N.; Coq, B.; Brotons, V.; Kumbhar, P. S.; Dutartre, R.; Geneste, P.; Bernier, P.; Ajayan, P. M. *J. Am. Chem. Soc.* **1994**, 116, 7935–7936. (d) Kong, J.; Franklin, N. R.; Zhou, C. W.; Chapline, M. G.; Peng, S.; Cho, K.; Dai, H. J. *Science* **2000**, 287, 622–625. (e) Robel, I.; Bunker, B. A.; Kamat, P. V. *Adv. Mater.* **2005**, 17, 2458–2463. (f) Correa-Duarte, M. A.; Pérez-Juste, J.; Sánchez-Iglesias, A.; Giersig, M.; Liz-Marzán, L. M. *Angew. Chem., Int. Ed.* **2005**, 44, 4375–4378. (g) Correa-Duarte, M. A.; Grzelczak, M.; Salgueirinho-Maceira, V.; Giersig, M.; Liz-Marzán, L. M.; Farle, M.; Sieradzki, K.; Diaz, R. *J. Phys. Chem. B* **2005**, 109, 19060–19063.
- (4) Shi, J. H.; Qin, Y. J.; Wu, W.; Li, X. L.; Guo, Z.-X.; Zhu, D. B. *Carbon* **2004**, 42, 455–458.
- (5) Lordi, V.; Yao, N.; Wei, J. *Chem. Mater.* **2001**, 13, 733–737.
- (6) Ravindran, S.; Chaudhary, S.; Colburn, B.; Ozkan, M.; Ozkan, C. S. *Nano Lett.* **2003**, 3, 447–453.
- (7) Fu, L.; Liu, Z. M.; Liu, Y. Q.; Han, B. X.; Hu, P. G.; Cao, L. C.; Zhu, D. B. *Adv. Mater.* **2005**, 17, 217–221.
- (8) Cao, J.; Sun, J.-Z.; Hong, J.; Li, H.-Y.; Chen, H.-Z.; Wang, M. *Adv. Mater.* **2004**, 16, 84–87.
- (9) Zhu, Y.-C.; Bando, Y.; Xue, D.-F.; Golberg, D. *J. Am. Chem. Soc.* **2003**, 125, 16196–16197.
- (10) Strano, M. S.; Dyke, C. A.; Usrey, M. L.; Barone, P. W.; Allen, M. J.; Shan, H.; Kittrell, C.; Hauge, R. H.; Tour, J. M.; Smalley, R. E. *Science* **2003**, 301, 1519–1522.
- (11) (a) Yu, W. W.; Peng, X. G. *Angew. Chem. Int. Ed.* **2002**, 41, 2368–2371. (b) Liang, H. J.; Angelini, T. E.; Braun, P. V.; Wong, G. C. L. *J. Am. Chem. Soc.* **2004**, 126, 14157–14165. (c) Tang, K. B.; Qian, Y. T.; Zeng, J. H.; Yang, X. G. *Adv. Mater.* **2003**, 15, 448–450.
- (12) Sheeney-Haj-Idia, L.; Basnar, B.; Willner, I. *Angew. Chem. Int. Ed.* **2005**, 44, 78–83.
- (13) (a) Liu, B.; Zeng, H. C. *J. Am. Chem. Soc.* **2004**, 126, 8124–8125. (b) Liu, B.; Zeng, H. C. *J. Am. Chem. Soc.* **2004**, 126, 16744–16746.
- (14) *Advanced Inorganic Chemistry*; Cotton, F. A., Wilkinson, G., Murillo, C. A., Bochmann, M., Eds.; Wiley-Interscience, New York, 1999; p 611.
- (15) Choi, J. Y.; Kim, K.-J.; Yoo, J.-B.; Kim, D. H. *Sol. Energy* **1998**, 64, 41–47.
- (16) Rieke, P.; Bentjen, S. B. *Chem. Mater.* **1993**, 5, 43–53.
- (17) (a) Liu, B.; Zeng, H. C. *J. Am. Chem. Soc.* **2003**, 125, 4430–4431. (b) Liu, B.; Zeng, H. C. *Langmuir* **2004**, 20, 4196–4204.